Scanning Microscopy Vol. 12, No. 1, 1998 (Pages 139-148) 0891-7035/98$5.00+.25
Scanning Microscopy International, Chicago (AMF O'Hare), IL 60666 USA

# A SCANNING FORCE MICROSCOPE COMBINED WITH A SCANNING ELECTRON MICROSCOPE FOR MULTIDIMENSIONAL DATA ANALYSIS

M. Troyon*, H.N. Lei, Z. Wang and G. Shang[1]

Groupe de Recherche Surfaces et Matériaux, Lab. de Microscopies Electronique et Tunnel 21, rue Clément Ader, 51685 Reims Cédex 2, France; [1]STM Lab., Inst. of Chemistry, Chinese Acad. of Sciences, Beijing 100080, China

(Received for publication July 30, 1996 and in revised form October 30, 1996)

**Abstract**

A scanning force microscope (SFM) intended for operation inside a scanning electron microscope (SEM) is described. This combined instrument allows one to image a sample conventionally by SEM and to investigate by SFM the local topography as well as certain physical characteristics of the surface (e.g., friction and elasticity). The combination of the two microscopes is very attractive because they complement each other in terms of depth of field, lateral and vertical resolution, field of view, speed and ability to image insulating surfaces. A multi-dimensional data space relative to the same area of a sample surface can be constructed, which should help to give new insights into the nature of materials.

**Key Words**: Scanning force microscope, scanning electron microscope, multidimensional data analysis.

*Address for correspondence:
M. Troyon
Universite de Reims Champagne-Ardenne
Lab de Microscop. Electronique et Tunnel
21, rue Clément Ader
51685 Reims Cédex 2, France
Telephone number: (33) 3 26 05 19 01
FAX number: (33) 3 26 05 19 00

## Introduction

The scanning force microscope (SFM) [3] has become an important surface analysis tool over the past few years. Its first function is three-dimensional topographic analysis with high lateral and vertical resolution; it is thus usable as a profilometer at the nanometre scale. In other respects, it is able to give information about certain physical properties of the surface since the tip is sensitive to different types of forces or interactions. Tribological investigations can be envisaged by recording the effects of lateral frictional forces [2]. It is also possible to study the visco-elastic properties [16], adhesion [6], magnetic [13] or electrostatic [19] characteristics of different materials. SFM is used not only in surface physics but also in various fields such as semiconductor development and biology. In spite of its advantages, mainly high resolution and the ability to image non-conductive samples, the use of the SFM is limited by its small scan area and slow scan speed.

The scanning electron microscope (SEM) is also a surface analysis instrument. SEM generally has a lateral resolution of about 5 nm, whereas a SEM equipped with a field emission gun has a resolution of about 1 nm. It must be pointed out that this resolution is obtained only in the case of very special test specimens capable of giving good contrast in the secondary electron imaging mode, gold particles on carbon for example. In most cases, specimens do not present sufficient contrast to be seen with the resolution limit of the instrument. The SEM has some other very interesting characteristics, mainly its large depth of field and the possibility of imaging large areas of a few $mm^2$ very quickly.

Scanning tunnelling microscopy (STM) is a technique closely related to SFM, with similar limitations (small scan area, slow scan speed). A few teams have tried to solve these limitations by combining the scanning tunnelling microscope with a SEM [8, 10, 11, 20, 22]. The STM/SEM hybrid instrument takes advantage of both techniques: the real-time image of the SEM makes it possible to view a wide field of the sample, choose a selected spot and then zoom onto that area with the STM. Nevertheless, our experience of the STM/ SEM combination showed us that the easy use of STM is restricted to very clean and well-conducting specimens. Very often, imaging reliability was not good, and tips broke because of contamination or poor conducting properties of the observed

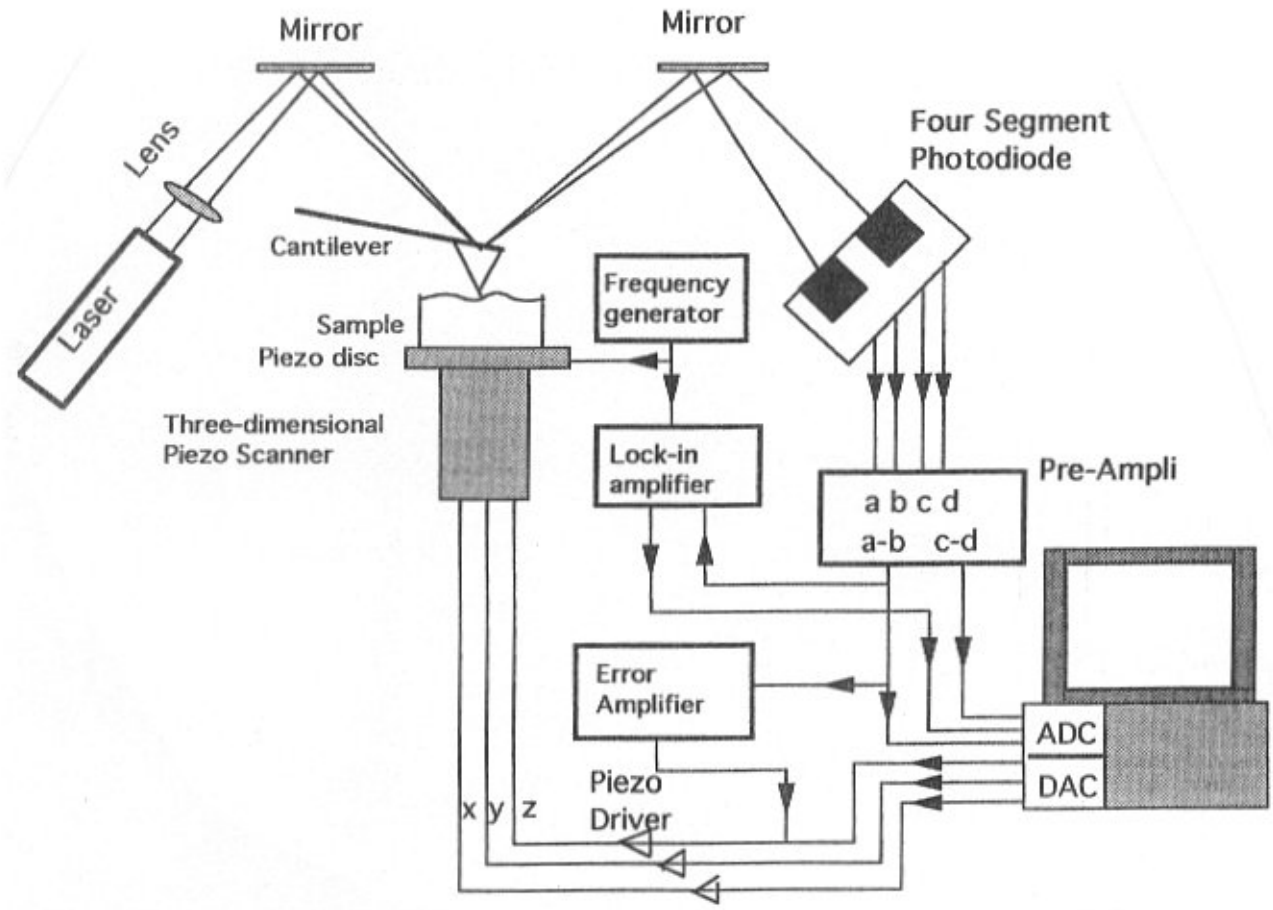


**Figure 1**. Schematic working principle of the SFM.

specimen.

As the SFM is able to image insulators, this draw-back is no longer a problem with a combined SFM/ SEM. SFM and SEM are, therefore, complementary techniques, the advantages of one compensating the draw-backs of the other. For the SEM user, besides improvements concerning the resolution (mainly the vertical resolution), a fundamental aspect is very attractive: SFM is able to provide multi-dimensional information from the surface (e.g., friction, adhesion, viscoelastic properties).

A few attempts have been made recently to combine a SFM with a SEM [7, 12, 18]. The system we have developed is based on the widely used technique of the position-sensitive detection of a laser beam from the cantilever. A commercial SFM/SEM using this method is available from Topometrix (Santa Clara, CA) but has not been described in the literature. In the present article, we describe the design of our combined SFM/ SEM and its performance, and we illustrate its potentialities with a few examples.

**SFM Description**

The basic principle of the SFM we have developed to be combined with a SEM is schematically explained in Figure 1. A 3 mW collimated laser diode (Melles-Griot) and a lens (focal length 25 mm) are rigidly mounted on a flange, which can be orientated to centre the focused beam on the cantilever top. Two fixed mirrors reflect the beam on a four-quadrant photodetector (Advances Photonics, Inc., Camarillo, CA), which can be moved in two perpendicular directions by means of a displacement mechanism. Topographic and lateral frictional force images can thus be simultaneously recorded. The piezo-electric ceramic (EBL#3, Staveley Sensors, Inc., East Hartford, CT) is a tube of 6.5 mm diameter giving a scanning area of 8 x 8 $\mu m^2$ and a Z dynamic range of $\pm$ 1.6 $\mu$m.

The viewing plane of Figure 1 is 45° tilted through with respect to the electron beam, that is, the specimen surface is also 45° tilted, facing the secondary electron detector (Fig.

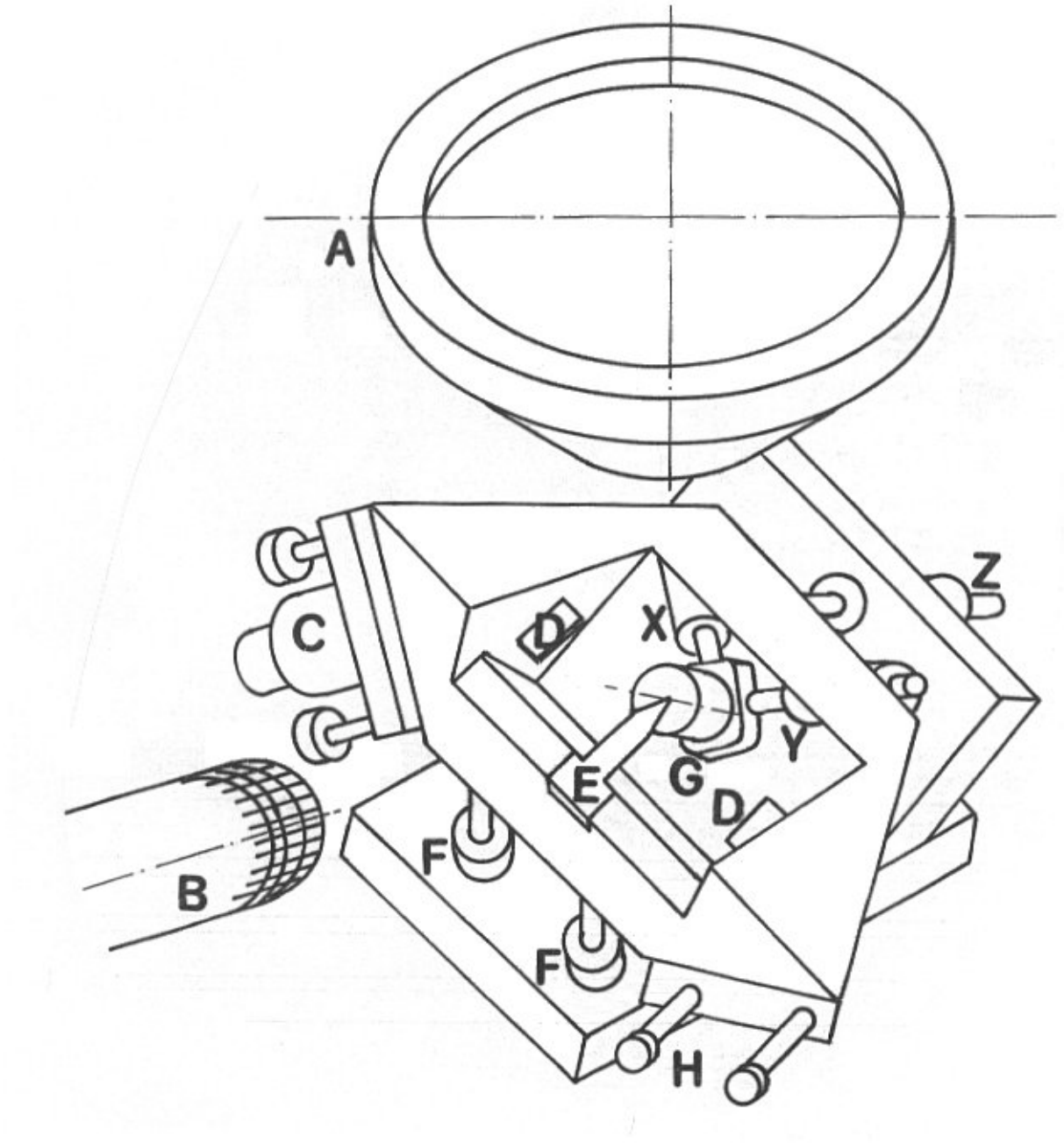


**Figure 2**. Schematic view of the SFM inside the SEM. (A) objective lens housing; (B) secondary electron detector; (C) laser diode; (D) mirrors; (E) cantilever support; (F) coarse approach screws; (G) piezo tube and sample; (H) photodetector adjustment screws; (X, Y, Z) stepper motors.

2). The specimen is placed at a working distance of 15 mm and a coarse positioner can move the specimen in the X and Y directions (± 1.5 mm) with two stepper motors ("inchworm"-type from Burleigh). The laser diode, the two mirrors, the cantilever, and the photodetector are all mounted in a support (the SFM head) that can be separated from the SFM base so as to change the specimen. The SFM head is set on three mobile axes, forming a tripod, and maintained by two springs.

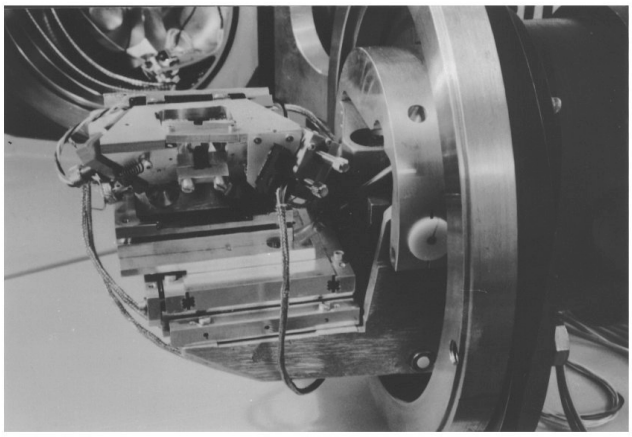

**Figure 3**. View of the SFM mounted inside the object chamber of SEM.

Two of these axes are threaded and can be manually rotated for a coarse positioning of the cantilever with respect to the specimen. The third axis is the sliding axis of a third inchworm motor, allowing one to engage the tip in contact with the specimen. The three motors are controlled from outside the SEM when the SFM head is under vacuum. Figure 3 shows the SFM mounted on the object chamber stage of a commercial SEM (Philips SEM 515, Eindhoven, The Netherlands). We have deliberately chosen to connect the SFM rigidly to the specimen displacement stage of the SEM even though the problem of mechanical vibrations is crucial in near-field microscopy for obtaining the atomic resolution. There are two reasons for this choice. In our previous experience of combining a STM to a SEM [20], we chose to support the STM head on a stack of 5 plates separated by viton O-rings to reduce the mechanical vibrations. This was efficient for obtaining the STM atomic resolution but was detrimental to the SEM resolution because the specimen was not laterally stable with respect to the column axis. Furthermore, we think it is illusory and thus, not useful, to strive towards atomic resolution in a SEM under conventional vacuum since high resolution studies require that the sample surface be prepared under ultra-high vacuum conditions to avoid any contamination.

The electronics are of analogue type and home-built on the basis of those developed by Radmacher [17]. The data acquisition, scan, display, processing and analysis are accomplished by a digital system (Macintosh Quadra 650, Apple Computer France, Cedex, France) equipped with two interface cards (Macadios GW1-625 and GW1-DAC, GW Instuments, Somerville, MA). The software, developed by H. Gaub's team (personal communication), allows simultaneous acquisition of three types of different signals: forward and backward scans are always recorded, and so six images of 256 x 256 pixels are obtained.

## Results and Discussion

The resolutions of the individual parts of the combined instrument have first been evaluated. Figure 4 shows the images of a classical test object regularly used to measure the SEM resolution (gold particles evaporated on carbon). Figure 4a is the SEM image taken at 30 kV. The resolution is evaluated to be of the order of 20 nm, which is the normal image quality of our SEM for a working distance of 15.9 mm; the presence of the SFM does not impair the SEM resolution. Figure 4b is the SFM image of these gold particles. Line profiling indicates that these are 2-3 nm high, which is a lower limit because the tip is too broad to reach into the space between granules. Nevertheless, the resolution is much better than that of the SEM. It is difficult to quantify it since gold particles do not present fine structures at their surface but they are clearly distinguishable, whereas some of these are only faintly visible in the SEM image. A STM rigidly connected to the specimen stage of a SEM has already been proven to be efficient for a good resolution [1]. Our own tests show also that this solution is a good one for a SFM/SEM combination. On the other hand, to verify the performance of our SFM, we tested it on an anti-vibration table in air; atomic resolution could be obtained on a mica sample.

The following example is presented to illustrate the interest of the combined SFM/SEM instrument and also to demonstrate the complementarity of the two techniques. Figure 5 shows that it is very easy to localize a particular spot of interest in a sample with the SEM, then to move the specimen under the probing tip and to zoom and reveal details by SFM that SEM is not able to show. Figure 5a is the SEM image of a two-dimensional grating made by electron microlithography. It consists of circular gold studs on a silicon substrate with a diameter of 200 nm and a periodicity of 400 nm. The top of the cantilever can also be seen in this image. The tip used is a conventional $Si_3N_4$ tip, the radius of which is approximately 40 nm. The tip height (4 μm) is not high enough to be visualized by SEM because it is hidden by the top of the cantilever. Unlike the case of the STM/SEM combination in the same configuration (tip 45° tilted with respect to the beam axis), the tip extremity cannot be seen, which is a small drawback. Nevertheless, it is easy to position the SFM tip on a detail when the latter has been located by SEM and then to correlate the resulting images. Figure 5b is the SFM image of a defect present in the grating. It reveals small structures on the stud surface that were not visible by SEM. One can also see that the studs appear as squares, whereas they are circular in the SEM image. This is an artefact due to the tip shape. Taking into account the stud height (80 nm), the sides of the tip (which has a pyramidal shape) have clearly been in contact

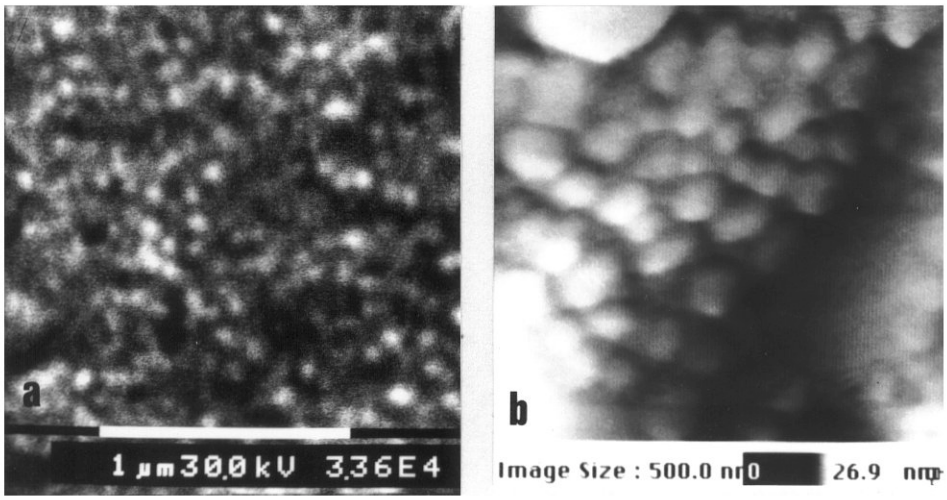


**Figure 4**. Images of gold particles evaporated on carbon obtained with the SFM/SEM combination. (**a**) Scanning electron micrograph; working distance = 15.9 mm; (**b**) topographical SFM image.

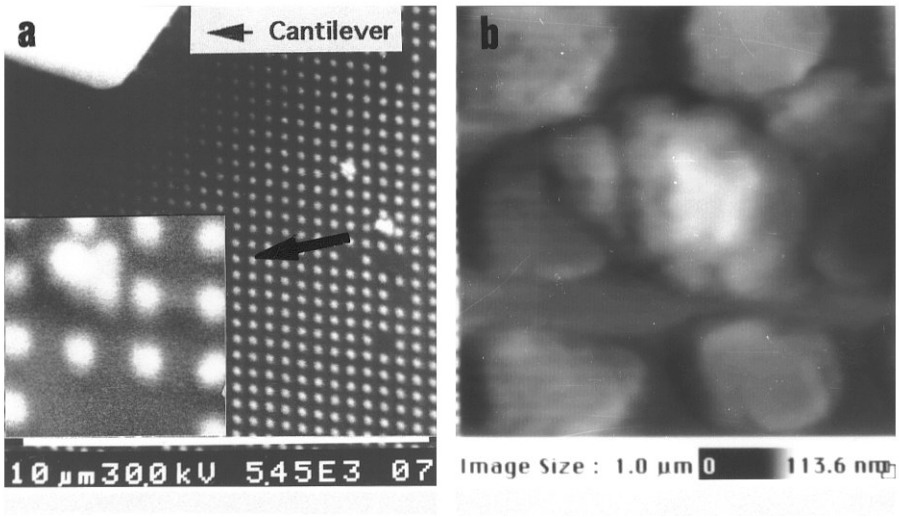


**Figure 5**. SFM/SEM images of a grating. (**a**) Scanning electron micrograph with the view of the cantilever and a small magnified defect; (**b**) Scanning force micrograph of the same small defect. The studs appear as squares. This is an artefact due to the SFM tip geometry.

with the studs. The image combines the information coming from the object and from the tip. This is the well-known "convolution" effect (the exact term is "dilation" in mathematical morphology [4]) between specimen and tip due to the finite dimensions of the latter. Observation by SFM alone of a relatively rough surface yields a wrong topographical interpretation, and this example demonstrates all the interest and complementarity of using both techniques together; SFM is the privileged tool to reveal fine structures and to measure heights precisely, whereas SEM is well-adapted to give a reliable lateral representation of rough objects.

The tribology of surfaces at the submicrometric scale can also be studied with our system. In order to measure frictional forces, we chose the fast scan direction perpendicular to the long direction of the cantilever. The cartography of the lateral forces and the topographic image are simultaneously recorded. For the moment, the information obtained is essentially qualitative but recent developments show that quantification at the nanometric scale of friction coefficients can be performed [14]. Figure 6a is the scanning electron micrograph of a ceramic sample composed of two phases: Al2O3, which is not conducting, and TiN, which is only slightly conducting. This material, used as a bioceramic, behaves under friction differently from alumina. Figures 6b and 6c are SFM images of the surface topography and frictional forces, respectively. The white areas of Figure 6c are characteristic of larger frictional forces. The information contained in both SFM images of Figure 6 provides better understanding of the SEM image contrast. The SFM topographic image tells us that the dark spots in the SEM image are in fact at a lower height level, and therefore one of the sample constituents may be preferentially pulled away by the mechanical

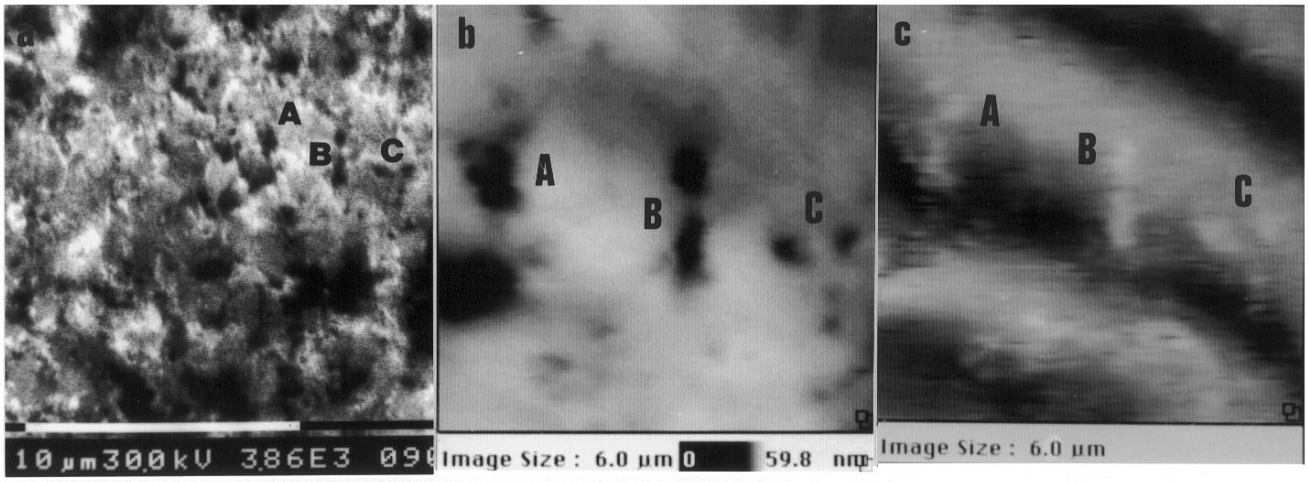


**Figure 6**. SFM/SEM images of a $Al_2O_3$TiN bioceramic (**a**) Scanning electron micrograph; (**b**) topographical, and (**c**) frictional SFM images. Areas labeled with letters A, B, C correspond in the topography image to areas with small heights (dark color), in the friction image to areas of high friction (light color).

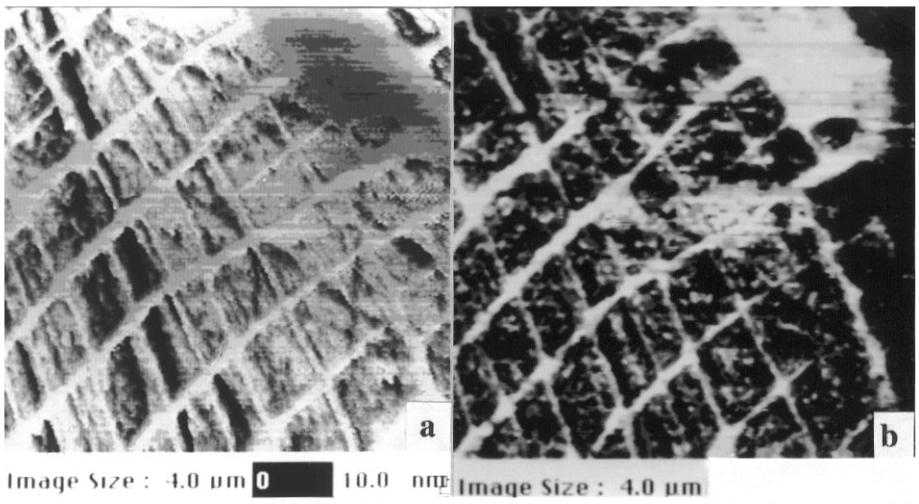


**Figure 7**. (**a**) Topography and (**b**) elasticity SFM images of a nickel based superalloy. The high frequency sample modulation displacement method is sufficiently sensitive to separate phases with close elastic moduli in a stiff material. The Young's moduli of the γ' phase (dark color) and γ phase (white color) are 115 and 130 GPa, respectively. The modulation signal amplitude is z = 2 nm, frequency f = 188 kHz and the cantilever stiffness k = 0.06 N/m.

polishing process. Some of these areas appear white in the frictional force image, showing that friction is more important there. Our SEM is not equipped with an X ray analyser, but X ray cartography would certainly help to determine which phase has the lowest friction coefficient.

Our SFM is also able to give information about the viscoelastic properties of materials thanks to a working mode called "sample displacement modulation." The sample is periodically moved up and down (Z wobble), and the tip response is measured with a lock-in technique. The sample is displaced by means of a transducer placed underneath the sample (Fig. 1). We used a small piezo-electric disk of thickness 0.5 mm. The frequency of the modulating signal must be chosen to be above the feedback response frequency (typically a few kHz). There are two different working regimes: below the cantilever resonance frequency (at low frequencies ~10 kHz) or well above it at high frequencies (between ~100 KHz and 1 MHz). The low frequency regime also called "the force modulation mode," is well adapted to soft materials such as biological ones [15, 16]. Measurement of the signal amplitude and phase gives the elasticity and viscosity response of the material, respectively [16]. The response of the cantilever to high frequency excitation is fundamentally different from its low frequency response. The theory of this regime has been developed by Burnham *et al*. [5]. Their analysis shows that modulating the position of the sample at

frequencies above the highest system resonance gives the clearest difference in cantilever response for the variations in elastic modulus of stiff samples. As the equations governing the cantilever behaviour at high frequencies are dominated by the acceleration, these authors named this working mode "Scanning Local-Acceleration Microscopy" (SLAM). Figure 7 is an example illustrating the capabilities of SLAM on a nickel-based superalloy single crystal. This material is composed of two phases γ and γ', whose elastic moduli are very close, 130 and 115 GPa, respectively [9]. The γ' phase consists of cubic precipitates, which appear as dark squares in the topographic SFM image of Figure 7a, since the single crystal was cut in slices with their main faces parallel to the (001) crystallographic plane [21]. The squares are slightly distorted because of hysteresis and non-linearity of the piezo-tube. After mechanical polishing (final step on 5O nm alumina powder), the γ' phase is revealed by dipping the sample for 15 seconds in a chemical solution that preferentially attacks the γ' phase. Therefore, the γ phase (the matrix) appears in white (the highest height level on the sample) and the γ' phase in black (the lowest level). The SEM image is not presented here because the γ' precipitate depths are so small, between 5 and 10 nm as revealed by the topographic SFM image, that there is absolutely no contrast in the image. Figure 7b is the SLAM image obtained from the amplitude response of the cantilever, with a modulation signal amplitude z = 2 nm, frequency f = 188 kHz and with a cantilever spring stiffness k = 0.06 N/m. The white areas in the image correspond to higher stiffness. The image shows clearly that the γ phase has a higher stiffness than the γ' phase. The latter does not appear completely homogeneous; some small white spots are present inside. These, which correspond to a higher stiffness, are presumably small γ particles pulled out during mechanical polishing, spread on the surface, still adhering to it and not removed during the short chemical etching. The high frequency sample displacement modulation method is so sensitive that "semi-quantitative" measurements of elastic moduli of stiff samples can be performed [23]; semi-quantitative is understood here as the possibility of measuring the elastic modulus of one of the constituent of a material relative to another constituent, the Young's modulus of which is known and used as reference.

We would like also to mention that there may be an additional advantage in performing SFM measurements or studies inside the vacuum of a SEM: the water layer that covers the specimen in air is desorbed under vacuum, and so there are no more capillary forces. Viscoelastic and adherence studies can therefore be performed quantitatively. All the studies using the non-contact resonant mode also take advantage of the low pressure because the Q-factor of the cantilever resonance is much higher. This has been demonstrated for a magnetic force microscope combined with a SEM [12].

## Conclusions

A scanning force microscope combined with a scanning electron microscope has been developed that has the possibility that a well-defined spot in a sample of a few $mm^2$ can be observed with the aid of an X-Y sample positioner using stepper motors of the inchworm type. These two instruments are complementary, the advantages of one compensating for the drawbacks of the other. Image correlation allows one to avoid some misinterpretations, relative to artefacts caused by tip-surface interactions in SFM or to contrast understanding in the SEM images. The presence of a SEM reduces the time and effort required in placing the SFM probe in the region of interest in a sample. From the point of view of the SEM user, the resolution is considerably improved and profilometry and roughness measurement at the nanometre scale thus become possible inside the SEM, with the SFM. The combination of these two techniques in the same instrument opens the way towards the construction of a multi-dimensional data space corresponding to the same place on the sample surface: the SEM gives access to information coming from secondary and backscattered electrons and allows X ray analysis to be performed, whereas the SFM, besides 3-D morphological analysis, allows nanotri-bological investigations (friction, wear, adhesion) and studies of some physical properties (viscoelastic, electric and magnetic) to be made.

With the multifunctional approach described, we believe that one can get new insights into the nature of materials and that such a SFM/SEM combination should become a practical tool in materials science, biology and in the semiconductor industry.

## Acknowledgements

We would like to thank Prof. H. Gaub for giving us the electronic circuit drawings and the image acquisition and processing software, Drs. A. Hazotte and S. Begin-Colin of Ecole des Mines of Nancy for supplying the nickel based superalloy and bioceramic $Al_2O_3$ TiN samples, respectively and M.E. Cambril for providing the periodic test specimen.

## References

[1] Asenjo A, Buendia A, Gomez-Rodriguez JM, Baro AM (1994) Scanning tunneling microscopy/scanning electron microscopy combined instrument. J Vac Sci Technol **B12**: 1658-1661.

[2] Bhushan B, Israelachvili JN, Landman U (1995) Nanotribology: Friction, wear and lubrication at the atomic scale. Nature **374**: 607-616.

[3] Binnig G, Quate CF, Gerber CH (1986) Atomic force microscope. Phys Rev Lett **56**: 930-933.

[4] Bonnet N, Dongmo S, Vautrot P, Troyon M (1994) A mathematical approach to image formation and image restoration in scanning tunneling and atomic force microscopies. Microsc Microanal Microstruct **5**: 477-487.

[5] Burnham NA, Kulik AJ, Gremaud G, Galto PJ, Oulevey F (1996) Scanning local-acceleration microscopy. J Vac Sci Technol **B14**: 794-799.

[6] Creuzet F, Ryschenkow G, Arribart H (1992) A new tool for adhesion science: The atomic force microscope. J Adhesion **40**: 15-21.

[7] Ermakov AV, Garfunkel EL (1994) A novel AFM/STM/SEM system. Rev Sci Instrum **65**: 2853-2854.

[8] Fuchs H, Laschinski R (1990) Surface investigations with a combined scanning electron-scanning tunneling microscope. Scanning **12**: 126-132.

[9] Ganghoffer JF, Hazotte A, Denis S, Simon A (1991) Finite element calculation of internal mismatch stresses in single crystal base super-alloy. Script Metal Mater **25**: 2491-2496.

[10] Gerber Ch, Binnig G, Fuchs H, Marti O, Rohrer H (1996) Scanning tunneling microscope combined with a scanning electron microscope. Rev Sci Instrum **57**: 221-224.

[11] Ichinokawa T, Miyazaki Y, Koga Y (1987) Scanning tunneling microscope combined with scanning electron microscope. Ultramicroscopy **23**: 115-118.

[12] Kikukawa A, Hosaka S, Honda Y, Koyanagi H (1993) Magnetic force microscope combined with a scanning electron microscope. J Vac Sci Technol **A11**: 3092-3098.

[13] Martin Y, Wickramasinghe HK (1987) Magnetic imaging by force microscopy with 100 nm resolution. Appl Phys Lett **50**: 1455-1457.

[14] Overney R, Meyer E (1993) Tribological investigations using friction force microscopy. MRS Bulletin **18**: 26-34.

[15] Overney R, Meyer E, Frommer J, Güntherodt HJ (1994) Force microscopy study of friction and elastic compliance of phase-separated organic thin films. Lang-muir **10**: 1281-1286.

[16] Radmacher M, Tillmann RW, Gaub HE (1993) Imaging viscoelasticity by force modulation with the atomic force microscope. Biophysical J **64**: 735-742.

[17] Radmacher M (1993) PhD Thesis. Kraftmikroskopie an weichen Proben. (Force Microscopy of Soft Specimens). Ludwig-Maximilians Universität München, Germany.

[18] Stahl U, Yuan CW, De Lozanne AL, Tortonese M (1994) Atomic force microscope using piezo-resistive cantilevers and combined with a scanning electron microscope. Appl Phys Lett **65**: 2879-2880.

[19] Terris BD, Stern JE, Rugar D, Mamin HJ (1990) Localized charge force microscopy. J Vac Sci Technol **A8**: 374-377.

[20] Troyon M, Lei HN, Bourhettar A (1992) Integration of an STM in an SEM. Ultramicroscopy **42-44**: 1564-1568.

[21] Troyon M, Hazotte A, Bourhettar A (1994) Modelling the AFM tip effect for quantitative analysis of precipitate volume fraction in nickel-based superalloys. Microsc Microanal Microstruct **5**: 489-499.

[22] Vasquez L, Bartolome A, Garcia R, Buendia A, Baro AM (1988) Combination of a scanning tunneling microscope with a scanning electron microscope. Rev Sci Instrum **59**: 1286-1289.

[23] Wang Z (1997) PhD Thesis. Développement d'un microscope à force atomique multifonctionnel associé à un microscope électronique à balayage. (Development of a multifunctional atomic force microscope combined with a scanning electron microscope). Université de Reims, Reims, Cedex 2, France.

## Discussion with Reviewers

**T. Ichinokawa**: Are there any problems taking SEM and SFM images upon the same area on a insulator material?
**Authors**: In SEM, insulators must be imaged at very low voltage to avoid charging effects. In that case, we did not encounter any problems when making SFM images. Even at higher voltages on partially insulating materials like $Al_2O_3$TiN (Fig. 6), we did not have difficulties.

**T. Ichinokawa**: Friction and viscoelasticity images may be changed by contamination.
**Authors**: Contamination may certainly change friction and adherence. On elasticity images, at least on stiff materials (like Ni-based superalloy in Fig. 7), it is unlikely that a small contamination layer, which should be much softer, has any influence because the instantaneous dynamic force is large at high modulation frequencies (several tens of nN). We did not see any differences between elasticity images taken in air before exposure to electrons and images taken in the SEM.

**M. Radmacher**: The laser beam in your design comes from the side of the cantilever; this will result in a deflection of the beam in the same direction by vertical forces (topography) as well as lateral forces (friction). In usual designs, the laser beam comes roughly from behind, which theoretically decouples the two effects. In practice, cross-talk between lateral and vertical forces can occur, and in your case, this crosstalk should be more pronounced. Are my concerns justified?
**Authors**: Theoretically, our design works correctly: lateral and vertical forces give two decoupled effects, the laser beam moves in two perpendicular directions on the photodetector. The only difference from the usual design is that the sensitivity for vertical forces is decreased approximately by a factor 1.3, but increased by the same factor for lateral forces. Consequently, if there is cross-talk between lateral and vertical

forces, and it certainly exists as in the usual design, this effect is slightly amplified in our case.

**M. Radmacher**: How do you interpret, in the friction data of Figure 6c, the bands of low friction force running roughly diagonal through the field of view?
**Authors**: We do not know. They might be due to a topographic effect because a depth line profiling in the topographic image reveals the presence of alternating grooves (depth around 15 nm) corresponding to the white and black bands in the friction image, or they might be due to surface contamination caused during the rotating mechanical polishing, which would increase the friction in the grooves.

**M. Radmacher**: We have recognized that force modulation data are prone to a plentitude of artefacts, possibly caused by crosstalk between topography or friction and modulation signal. Have you tried to rule out these artefacts in the data presented here? Since your sample shows ridges, I would be concerned about the addressed artefacts.
**Authors**: In the present case, the resolution is low (1 pixel = 15 nm), the height differences on the surface are small (5-10 nm) compared to the tip radius (50 nm), and the friction coefficients of the two phases are very close to each other; consequently, it is very unlikely to see artefacts like this.

**M. Radmacher**: What scientific questions do you want to access now? What new information, not obtainable with the single instruments, do you want to gain?
**Authors**: In the near future, we are interested by two kind of studies for which the SFM/SEM instrument can help: (1) problem of adhesion of silane between fiberglass and epoxy matrix. The SEM would provide the different scales of the heterogeneous distribution of silane layer over a large field of view, and the SFM in the friction mode and elasticity mode would help to estimate the nature and properties of the objects adsorbed on the surface; (2) study of thermoelasticity properties of materials. The modulated beam will provide the energy to heat the sample locally and cause an elastic deformation measured by the SFM and analysed with a lock-in technique.

**A.M. Baro**: The data of Figure 5 are very frustrating, since SFM images are worse than SEM images, and these data are an argument against using such a combination. They are also in contradiction with the argument given by the authors that SFM/SEM combination is a much better choice than STM/SEM. In the last case, the shape of the studs is preserved as reported in the paper by Gomez-Rodriguez JM *et al*. (1989) Ultramicroscopy **30**: 355.
**Authors**: Figure 5 illustrates the possibility of artefacts in the SFM images caused by geometrical effects of the tip when surfaces are very rough. These tip effects are also present in STM, as outlined in the paper referred to by the reviewer. Their importance is related to the tip shape and size. In the case of rough surfaces, the SEM gives a better resolution, and thus our example illustrates well the complementarity of the two instruments. In our opinion, and in contrast to the reviewer's assertion, this is an argument for using such a combination. We believe that SFM/SEM combination is a better choice than STM/SEM, mainly because of surface conductivity problems; with the SFM, insulators can be imaged, plus all the other information that the SFM can give: elasticity, friction, etc.

**Reviewer V**: The idea of combining a scanning probe microscope (SPM) and a SEM in one instrument is actually relatively old. Topometrix launched the Observer™ which was originally designed for the Hitachi 4000 series but is now available for two or three other SEMs. Today, the Observer™ is used for standard quality control in the semiconductor industry as well as in hard drive manufacturing. For obvious reasons, there are no publications available from these industries. According to Topometrix, the Observer™ is also used in academic research. Besides, OMICRON Vakuumphysik GmbH (Germany), commercially offers the MULTISCAN LAB, which combines the STM and SEM. Furthermore, Digital Instruments (Santa Barbara, CA) commercially offers the Dimension™ 5000 which is capable of three-dimensional imaging areas up to 35 cm, which makes the use of the much more complex and probably more expensive SEM obsolete, if used only to navigate the SPM tip or to get an overview on large scales. Park Scientific Instruments (Sunnyvale, CA) builds commercial SPM in ambient air which are by default combined with an optical microscope, and the instrument is capable of producing continuous 3D information from nm-scales (SPM) to cm-scales (optical microscope).
**Authors**: The idea of combining STM and SEM is effectively 10 years old, but, concerning AFM/SEM combination, only three papers have been published on the subject, to our knowledge. A commercial instrument is available on the market but design and performance of the system has not been published. What is the resolution of the AFM inside the SEM; what becomes of the SEM resolution? Only the users of this system know. In electron microscopy, manufacturers publish the performance of their microscopes. Topometrix did not for this system. The interest of the SEM in the AFM/SEM combination is not only linked to the fact that it is easy to navigate the SFM tip or get an overview on large scales: the SEM in many cases will have a better lateral resolution than the AFM. Indeed, the probe size of a SEM equipped with a field emission gun can be smaller than 1 nm, compared with the best AFM tips which have a radius of about 10 nm; the example we have given of artefact produced by the AFM tip demonstrates the interest of image correlation. SEM also has its own fields of competence (large field of view, backscattered

electron detection, X ray analysis, etc.) that the others (Dimension™ 500, SPM/optical microscope combination) do not have.

**Reviewer V**: The authors write that they have rigidly connected the APM head to the SEM stage to preserve the SEM resolution. To my knowledge, the previously built instruments do not considerably hamper the SEM resolution as long as there is a different translation proper connection to the mass. Also, the use of a different cantilever (not piezo-resistive) or a different translation stage is not original; it has been realized with similar designs under ambient conditions as well as in ultra-high vacuum and has nothing to do with the combination SPM/SEM.

**Authors**: If we refer to the three previous papers concerning AFM/SEM combination, one of the AFM designs [12] is based on an antivibration stack of plates separated by a viton O-ring. We know by experience that this solution is detrimental to the SEM resolution. In the two other papers [7, 18], the AFM head is rigidly connected to the SEM state, and the AFM design does not allow the coarse X, Y positioning of the specimen with respect to the tip. None of these three papers shows the resolution of the SEM and AFM when they are combined; only low magnification images are presented. To construct an AFM head which allows the position of the specimens with respect to the tip to be in X, Y, and Z directions from the outside of the SEM is not a trivial problem; it is certainly more complicated than constructing a STM head because of the presence of a centerable laser diode and photodetector and mirrors. We believe one of the merits of our paper, although the idea of combining SFM and SEM is not original, is to demonstrate with resolution tests the performance of such a combined instrument. We also believe that it is useful to give a full description of the design philosophy and examples showing the interest of such an hybrid SFM/SEM instrument, since these combined microscopes are relatively new and uncommon in laboratories doing academic research.